Designing Multistage Frac Packs in the Lower Tertiary Formation—Cascade and Chinook Project

Ziad Haddad, FOI Technologies, SPE; **Mike Smith,** NSI Technologies, SPE; and **Flavio Dias De Moraes,** Petrobras, SPE

Summary

The Cascade and Chinook Project is located in the Walker Ridge area in the Gulf of Mexico (GOM), 250 miles south of New Orleans in depths between 8,200 and 8,900 ft. The oil-producing reservoir is in the Lower Tertiary Wilcox formation, with a gross sand thickness of 1,200 ft. The reservoir midpoint is at an average depth of 25,600 ft true vertical depth subsea (TVDss), with a bottomhole pressure of 19,500 psi and a bottomhole temperature of 260°F. The reservoir comprises vertically stacked thin beds of sand and fine-grained-siltstone intervals with effectively no vertical permeability. Additional information on this project can be found in Moraes et al. (2010).

Multiple limitations were considered during the initial design phase of the frac-pack program. The fracs were designed taking into account the use of a single-trip multizone (STMZ) sand-control system. Some of these design challenges are briefly discussed by Cunha et al. (2009). Although this system was not crucial in the overall implementation of the frac program, it added additional complexity from an operational standpoint because of a continuous, multistage frac operation. Some of the operational limitations included service-tool erosion limitations because of maximum pump rates and proppant volumes, overall frac-vessel capacity, boat-to-boat fluid transfers, and crew fatigue. The geological complexities of the reservoir were another major challenge in completing this very thick interval. Perforation intervals had to be placed to avoid a fault (and thus a potential early screenout), avoid a water contact, comply with tool-spacing limitations, and still maximize contact with net pay.

This paper addresses the approach taken to develop a fracture-stimulation program for the Lower Tertiary formation in the Cascade and Chinook Project. Some of the major questions addressed during this process include the following: How many fracture treatments are needed? What is the optimum fracture geometry? What is the desired conductivity? How to effectively position the perforation intervals? What is the desired pump rate, and is a high-density fluid needed to fracture this deep, high-pressure formation? The approach, the answers, and the treatment are discussed along with responses to additional questions that arose during the actual fracturing operations.

Along with the Lower Tertiary in the GOM, the industry faces similar challenges around the world. These include reservoirs with potentially large reserves but much lower permeability (caused by depth and in-situ stresses) where fracturing is required for both stimulation and potential formation-collapse sand control. Careful planning is necessary to avoid costly learning curves in these environments.

Introduction

At the beginning of the process of conducting feasibility studies and the preliminary treatment designs for what is considered to be one of the deepest fracture treatments in the history of the industry (Halliburton Energy Services 2011), there were no existing data or any history on the Lower Tertiary for guidance. The only frac data available from the Lower Tertiary were those of the Jack Well Test (Jack 2 well) conducted by Chevron in 2006. Although the data from the Jack Well Test were partially used to formulate the "basis of design" for the Cascade and Chinook Project, they are not discussed in this paper because the data remain confidential. Furthermore, most of the experience in the GOM was geared toward pumping frac packs in high-permeability formations such as the Miocene formation for the primary purpose of sand control. We recognized early on that the mindset had to change when dealing with the Lower Tertiary formation. The focus had to be shifted from a "soft rock" frac-pack completion to a "hard rock" hydraulic-fracturing completion similar to what is done in the Wilcox formation in south Texas. This type of hard-rock fracturing is discussed by Britt et al. (2006). The secondary objective was to design a sand-control completion for the primary purpose of retaining the proppant pack and eliminating the all too familiar problem of proppant flowback in "screenless" hard-rock fracturing completions.

We set out to develop a process that outlines an initial procedure for developing a basis of design for future Cascade and Chinook hydraulic-fracturing treatments. The general goal of this initial planning phase was two-fold: (1) to develop a complete and comprehensive set of fracture-treatment design data to be used in developing the preliminary treatment designs and evaluation of material-selection options and (2) to identify key questions for future wellsite data collection and execution.

The following is the outline that was used to develop the fracturing program:

1. Rock mechanics.
   - Review and compile all existing stress data including past fracture treatments and leakoff-test data.
   - Review existing rock-mechanics laboratory data, and determine core availability for future testing.
   - Define critical data needed.
   - Select core take points for additional core tests (stress/strain over a range of confining pressures).
   - Stress/strain testing for failure envelope, residual grain-size distribution after failure for screen sizing (if needed).
   - Conduct proppant-embedment study on cores (sand and shale) under high confining stresses to simulate reservoir depletion.
   - Develop a local correlation to convert the dynamic Young's modulus to a static Young's modulus
2. Materials.
   - Frac Fluids.
     - Gather details and history of frac fluid used on the Jack Well Test.
     - Define required fluid testing protocol.
     - Evaluate the need for shear-history testing of crosslinked-borate systems.
     - Determine compatibility testing with cores and formation fluids.
     - Evaluate advantages and disadvantages of using a weighted fracturing fluid.
       - Determine long-term stability of fluid rheology.
       - Review available data from service-company information.
       - Review case histories where weighted fluid systems were used.

This paper (SPE 140498) was accepted for presentation at the SPE Hydraulic Fracturing Technology Conference and Exhibition, The Woodlands, Texas, USA, 24–26 January 2011, and revised for publication. Original manuscript received 10 March 2011. Revised manuscript received 7 December 2011. Paper peer approved 19 December 2011.

TABLE 1— AVERAGE FORMATION PROPERTIES

Variable	Estimated Value
Formation Depth	25,100 ft TVDss
Water Depth	8,143 ft
Formation Thickness	Wilcox 1 – 400 ft TVD Wilcox 2 – 600 ft TVD (to water contact)
Porosity	16% to 20%
Permeability, k	Wilcox 1 – 10 to 110 md, $k_{Avg} \approx 25$ md Wilcox 2 – 2 to 30 md, $k_{Avg} < 10$ md
Reservoir Pressure	19,300 psi at 25,500 ft TVD – 0.75 psi/ft
Fluid loss height, H_l	Assume all sand is fluid loss H
Fluid loss coefficient, C	Wilcox 1 – 0.004 ft/√min Wilcox 2 – 0.003 ft/√min
Young's Modulus, E	2 to $3X10^6$ psi – Sand & Shale 6 to $8X10^6$ psi – Thin "Hard" Streaks
Poisson's Ratio	0.25 to 0.27
In-situ stress	Sand – 0.77 psi/ft Maximum stress difference between sand/shale layers, 100 psi (i.e., < 0.01 psi/foot of depth TVD)
Formation Temperature	260 °F
Deviation over Perfs	17 deg

□ How beneficial are they in reducing the treating pressure at high pump rates?

□ Can the use of such fluids be ruled in/out before the start of the completion program?

- Proppant.

■ Review stress and temperature conditions for long-term production with respect to type and size of proppant desired.

■ Determine if special testing is needed.

3. Design approaches.

- STMZ system (four or five fracs with short perforation intervals).
- Multitrip multizone (MTMZ) conventional system (three fracs with longer perforation intervals).
- Build a matrix to present results of simulation runs for STMZ vs. MTMZ [e.g., perforation interval, frac height, X_f, K_fW, skin, productivity index (PI)]

4. Sand-control issues.

- Determine the formation grain-size distribution.
- Determine the need for special products to prevent fines migration.

5. Wellbore-volume effects.

- Evaluate bullheading vs. spotting fluids.

6. Tool movements.

- Determine the maximum anticipated cool-down temperatures.
- Optimum weight-down and effects on work-string buckling.

Design Challenges

The first well that was completed was Well A in the Cascade field in the Lower Tertiary (Wilcox) formation with three propped-fracture treatments in the upper and lower Wilcox zones. Typical formation properties are included in **Table 1,** with an openhole-log section illustrated later in this paper. The challenge was to complete this very thick interval while avoiding fracturing into the oil/water contact and avoiding placing perforations near a fault at 25,832 ft measured depth (MD).

Major questions addressed for the preliminary design include: How many fracture treatments were needed? What would be the desired fracture half-length and conductivity? What would be the optimum perforation length and locations? What would be the desired pump rate, and was weighted frac fluid needed to fracture this deep, high-pressure formation?

The prefrac stress testing and the post-frac history matching mentioned in this paper were from the Cascade field only. A similar approach was used to develop the fracturing program for the Chinook field.

Completion Hardware. An STMZ sand-control completion system was selected for the Cascade and Chinook Project. The technology of the STMZ system is not new to the industry. It has been used successfully in much shallower completions (less than 15,000 ft) and at much lower bottomhole pressures. This was the first time that this type of technology was used at depths, pressures, and operating conditions such as those in the Cascade and Chinook Project (Baker Hughes 2011).

Reservoir modeling indicated that hydraulic fracturing was required to produce the wells at economic rates. Given the overall gross thickness of the Lower Tertiary reservoir (more than 1,200 ft), each well would require multiple-stage fractures to stimulate the entire reservoir effectively. Conventional stacked frac packs were considered initially because of the extensive industry experience using this type of technology in the GOM. It was anticipated that it would take 30 days and eight round trips to install a conventional three-zone stacked frac pack vs. 14 days and three round trips for a five-zone STMZ system. Ultimately, an STMZ system was selected as the primary sand-control completion system for its significantly shorter installation time and cost savings. Although the STMZ system was not essential for achieving the desired stimulation program, it added complexity, which adversely affected the execution.

This paper does not detail the deployment and use of the STMZ system but briefly discusses its effects on the design and execution of the frac jobs. Additional information on the STMZ system is discussed by Ogier et al. (2011). Although this technology is still considered new to the Lower Tertiary and similar deep reservoirs, we believe that it is a step in the right direction to ensure an efficient and less-risky completion.

Perforation Designs. The perforating philosophy also had to change. The perforating intervals were now considered as a means to "initiate" a fracture and take advantage of the in-situ stresses to achieve the optimum geometry. This is discussed by Lestz et al. (1999). Again, the usual mindset had to change from perforating all the net pay in soft-rock formations to limiting the perforation intervals and relying on the fracture geometry to contact all the pay intervals. Data on the perforating-gun system (charge type, shot density, phasing) can be found in Sanders et al. (2011).

Two simulation runs in the Wilcox 2 sand of a Cascade exploration well were performed to demonstrate the effectiveness of properly positioning the perforation interval to take advantage of the in-situ stresses. Both cases were simulated with a gridded, planar 3D fracture simulator using the same stress profile, pump schedule, and pump rate. **Fig. 1a** was simulated by positioning the perforations at the top of the interval, which resulted in an upward "height growth" into the shale section and part of the lower Wilcox 1 sand while leaving the lower

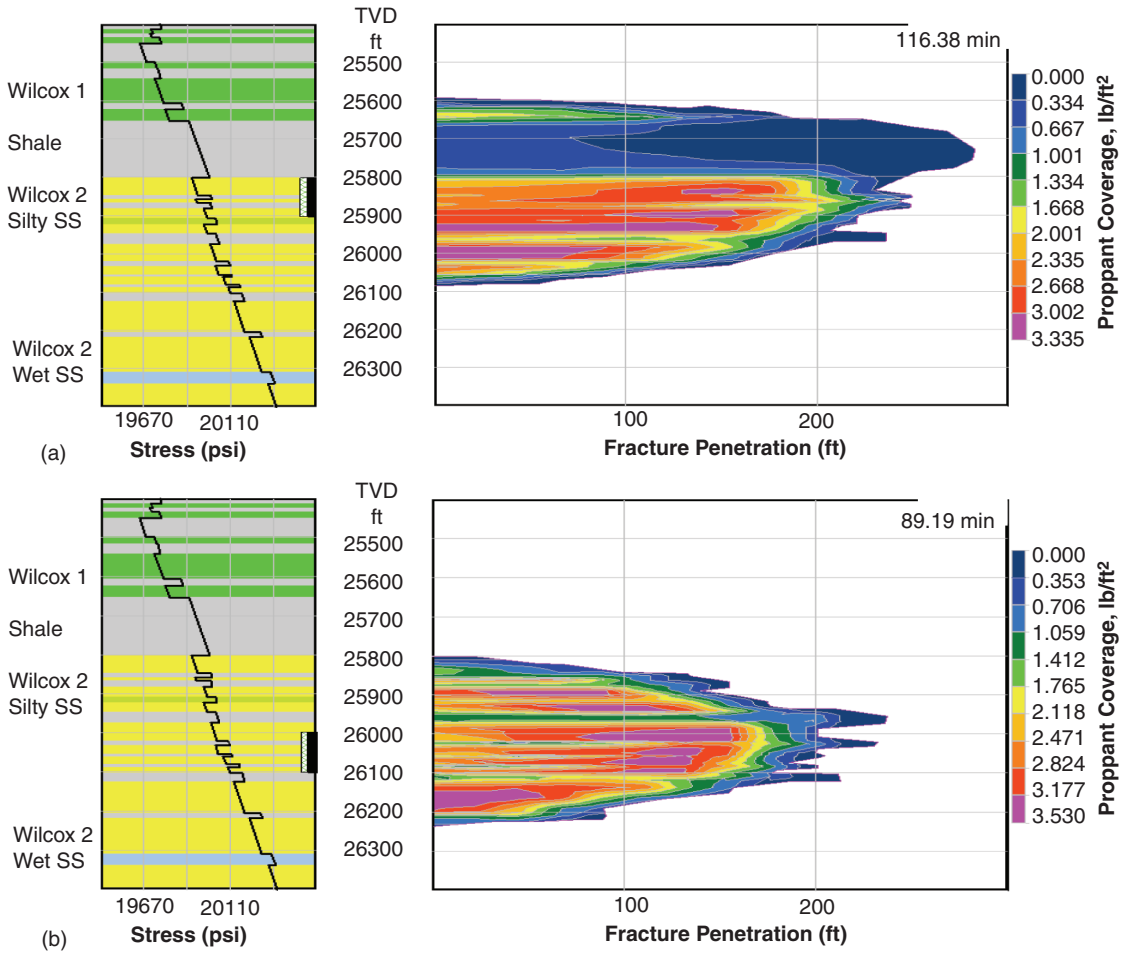

Fig. 1—Perforation-placement example.

part of the Wilcox 2 sand unstimulated. On the other hand, Fig. 1b was simulated by placing the perforations lower within the interval, resulting in more desirable fracture geometry across the Wilcox 2 sand.

To accommodate the STMZ system, the entire Wilcox formation had to be perforated in a single gun run. This approach added additional complexities to the overall fracturing program because it eliminated the option of modifying the perforating intervals up the hole, as the case would be with a stacked frac-pack completion, if results dictated it after the initial frac stage.

Operational Limits. In addition to the previously mentioned limitations, specific operational limits for the Cascade and Chinook fracturing program were determined and included the following:

- Maximum stimulation-vessel capacity
  - 1,500,000 lbm of 20/40 US-mesh bauxite proppant
  - 6,200 bbl of 8.7 lbm/gal fluid
  - 30,000 gal of acid
- Service-tool erosion limits
  - 40 bbl/min
  - 1,500,000 lbm of 20/40 US-mesh bauxite proppant
- Frac-pack completion-equipment spacing
  - 120 ft of MD desired between perforated intervals to house the completion equipment
- Logistics
  - Can the vessel be resupplied with fluid and proppant on location?
  - Safety of personnel when conducting boat-to-boat transfers
  - Crew fatigue from continuous operations
  - Weather

Geological Complexities. Another uncertainty identified was the potential risk of exceeding the weight of the overburden (presumably the vertical stress) and creating multiple competing fractures near the wellbore or, even worse, a horizontal fracture. This result would have been detrimental to the productivity of the well because the objective of hydraulically fracturing this highly laminated formation with zero vertical permeability was to allow the fracture to grow beyond the perforation interval and contact additional pay. Ultimately, we took a calculated risk relying on experience from completing similar hard-rock formations in south Texas where high reservoir pressure and high in-situ stresses frequently lead to treating pressures very near (or above) overburden stress. These data are discussed by Gil et al. (2007).

Moreover, geologic limits (log interval in **Fig. 2**) included the following:

- How to effectively treat the entirety of this thick interval.
- Avoid perforating near a major fault at 25,832 ft MD.
- Avoid the oil/water (O/W) contact at 26,357 ft MD by preventing the fracture from propagating below 26,250 ft.

Preliminary Design Recommendations

Desirable Fracture X_f and K_fW. Pseudosteady-state "folds-of-increase" calculations were used to give a preliminary estimate of the desired fracture length/conductivity. This type of analysis is discussed by Meyer and Jacot (2005). These calculations used values for net pay and permeability from Petrobras' petrophysical analysis. The initial results, presented as a normalized PI (BOPD/psi drawdown) based on an oil viscosity of 20 cp, are summarized in **Fig. 3.** This suggests a desirable fracture of 150 ft 1/2-length, with more than 2 lbm/ft^2 proppant coverage using high-strength bauxite proppant. This would provide three times the deliverability of an unstimulated well. Assuming simple radial fracture geometry, this implies a job size of 170,000 lbm of proppant for each fracture treatment with three to four treatments needed to stimulate the entire formation thickness.

Fluid-Loss Coefficient. Fluid loss is one of the most important variables in hydraulic fracturing. It is also a complex variable influenced by the formation permeability, relative permeability to

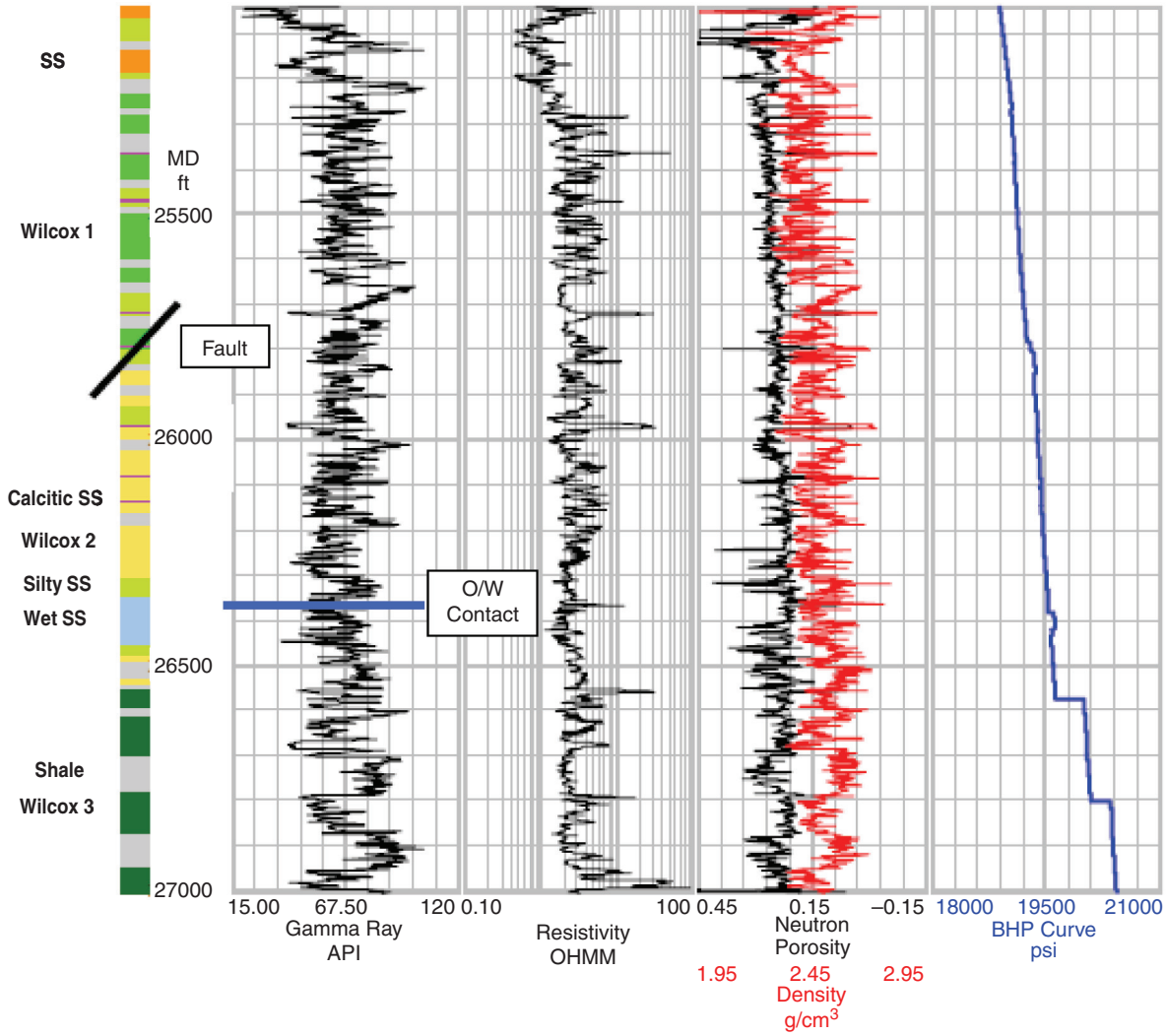

Fig. 2—Cascade Well A, Wilcox formation.

the leakoff fluid, reservoir-fluid properties, and filter-cake properties of the fluid. The importance of this variable is discussed by Lacy (1997). Filter-cake behavior is measured in the laboratory as a fluid-loss-control coefficient C_W with units of ft/√min. Given the expected permeability in the Wilcox formation, fluid loss is expected to be fairly low because of the reservoir-fluid viscosity. A viscosity of 20 cp was used as an example to generate the results in **Fig. 4.** To determine the fluid-loss-control performance of the gel filter cake, C_W, laboratory tests were run using 35 lbm/1,000 gal borate crosslinked gel (Fig. 4a) and 35 lbm/1,000 gal linear gel (Fig. 4b) on actual core samples from the Cascade field. This shows a C_W of approximately 0.003 ft/√min for the crosslinked fluid. As anticipated, no filter cake was formed for the linear gel.

These values, along with formation properties and reservoir-fluid values, were used to calculate a total fluid-loss coefficient C_T for the 35 lbm/1,000 gal crosslinked gel. This is seen in Fig. 4c for various values of formation permeabilities. This suggests a value of approximately 0.001 to 0.002 ft/√min for the Wilcox 2 and a slightly higher value of 0.002 to 0.003 ft/√min for the higher-permeability upper Wilcox 1. Higher values of 0.003 and 0.004 ft/√min were used for the preliminary designs.

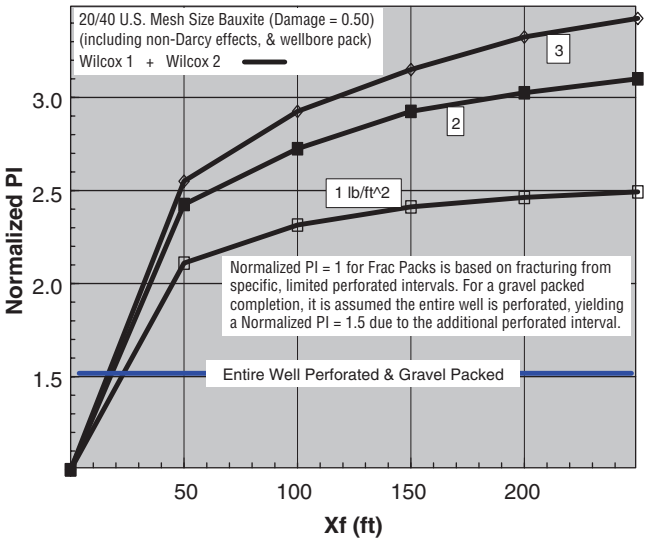

Fig. 3—Post-frac PI.

Young's Modulus. Young's modulus is a measure of the "stiffness" of a formation and is considered a major variable in determining fracture width and controlling net pressure inside the fracture. The importance of this variable is discussed in detail by Smith et al. (2001). A hard rock (i.e., high modulus) causes net treating pressure to be high, and thus makes fracture-height growth more likely. The best source of Young's modulus data is stress/strain tests conducted on core samples.

A few stress/strain tests for Young's modulus were available from earlier studies, along with several uniaxial pore-volume-compressibility tests **(Fig. 5a).** For these, a core sample is compressed axially while simultaneously increasing the lateral confining pressure to maintain zero lateral expansion. This type of test is discussed by Britt et al. (2004). Though this is a different stress path from a normal test for Young's modulus, a value for Young's modulus can be derived from these test results. In addition to these data, in preparation for

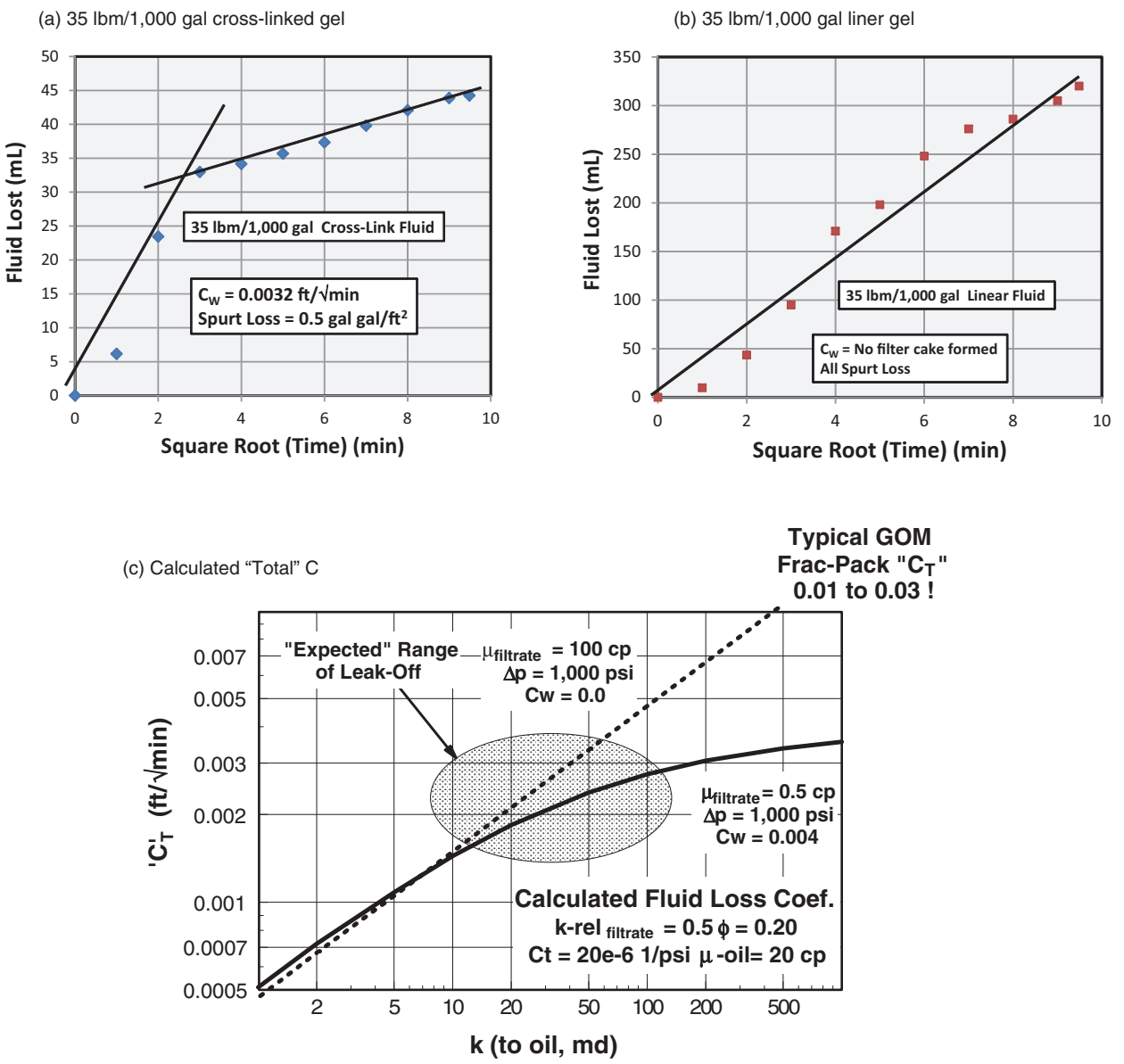

Fig. 4—Laboratory fluid-loss test results.

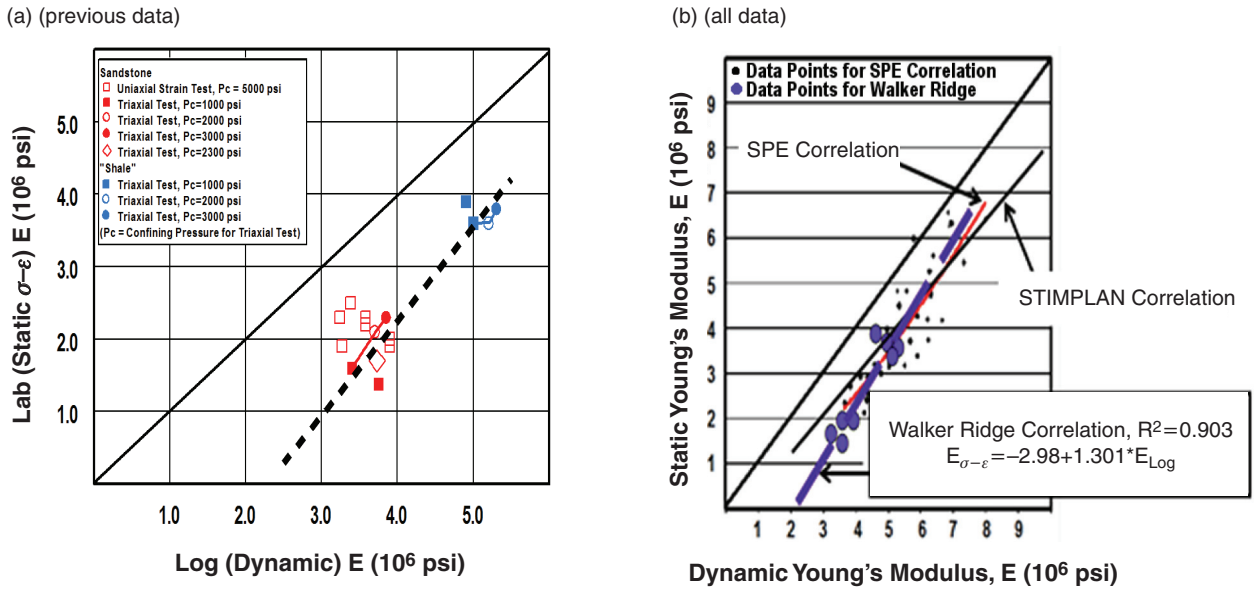

Fig. 5—Laboratory stress/strain-test results.

TABLE 2—NEW STRESS/STRAIN-TEST RESULTS (CASCADE FIELD)						
Sample	Depth (MD ft)	Young's Modulus (MM psi)	Poisson's Ratio	Confining Pressure (psi)	Sample Lithology	Porosity
A	26,314.30	3.92	0.31	1,000	Shale	0.11
B	27,122.75	1.38	0.3	1,000	Sand	0.21
C	27,135.30	1.59	0.27	1,000	Sand	0.2
C	27,135.30	2.12	0.25	2,000	Sand	0.2
C	27,135.30	2.33	0.2	3,000	Sand	0.2
D	27,645.20	3.59	0.29	1,000	Shale	0.12
D	27,645.20	3.59	0.2	2,000	Shale	0.12
D	27,645.20	3.81	0.14	3,000	Shale	0.12

the Cascade Well A fracture treatments, new stress/strain tests (and corresponding laboratory sonic-velocity measurements) were conducted by NSI Technologies on sand and shale samples (**Table 2**) obtained from offset exploratory wells in the Cascade field.

These data were used to derive a static/dynamic modulus correlation (Fig. 5b). This was then used with dipole sonic logs to generate a geomechanical stress profile for the Wilcox formation. This type of correlation is discussed by Lacy (1997).

Proppant Embedment. Given the geology of the Wilcox formation, the fracture treatments will have to penetrate and prop open a fracture through shale layers. This makes proppant embedment **(Fig. 6a)** a major concern because the proppant pack will be subjected to high drawdown pressures during the life of the well, potentially reducing the conductivity. Thus, laboratory embedment tests (Fig. 6b) were conducted on sand and shale samples from the Cascade field to better understand the effects of proppant embedment

(a) Embedment Testing Schematic

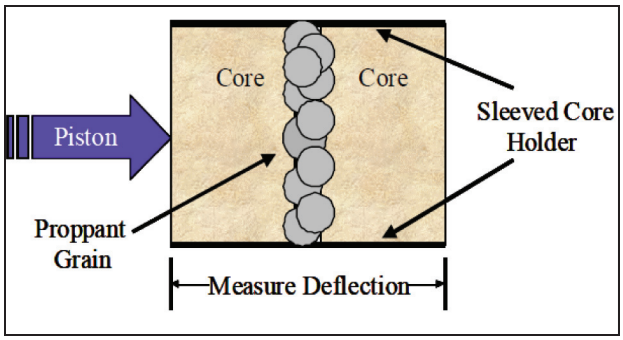

(b) Scanning Electron Microscope (SEM) Image of a Proppant Embedment Test

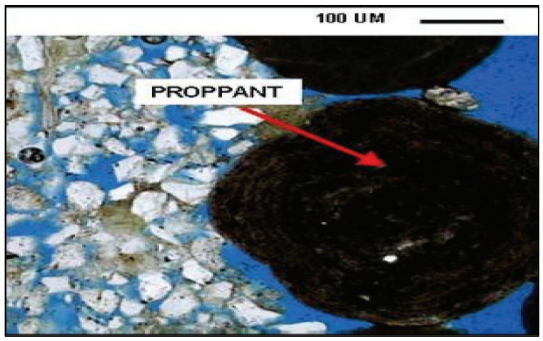

(c) Shale Sample at 27,645.20 ft (Embedment Graph and Picture)

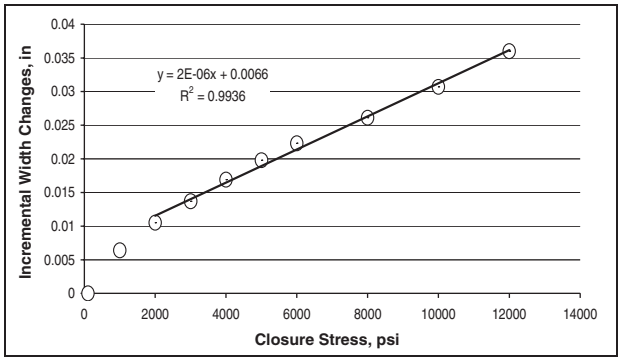

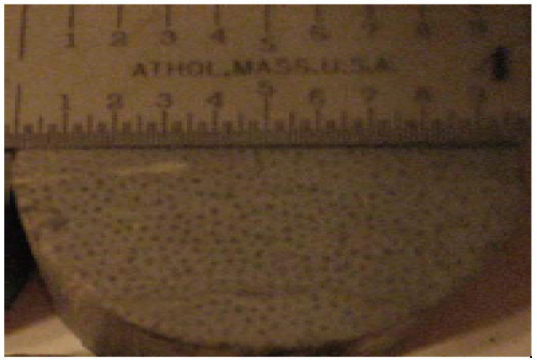

(d) Sand Sample at 27,135.30 ft (Embedment Graph and Picture)

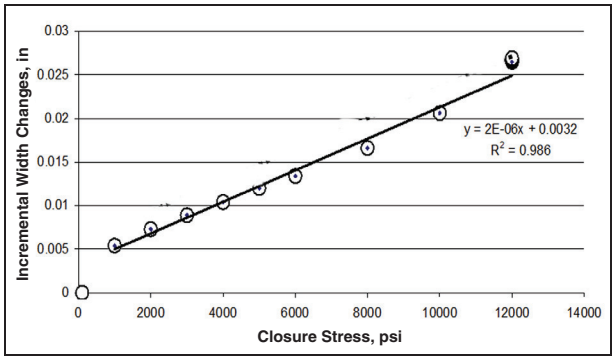

Fig. 6—Proppant-embedment-test data (Cascade field).

(a) Cascade Exploration Well Simulation Treatment

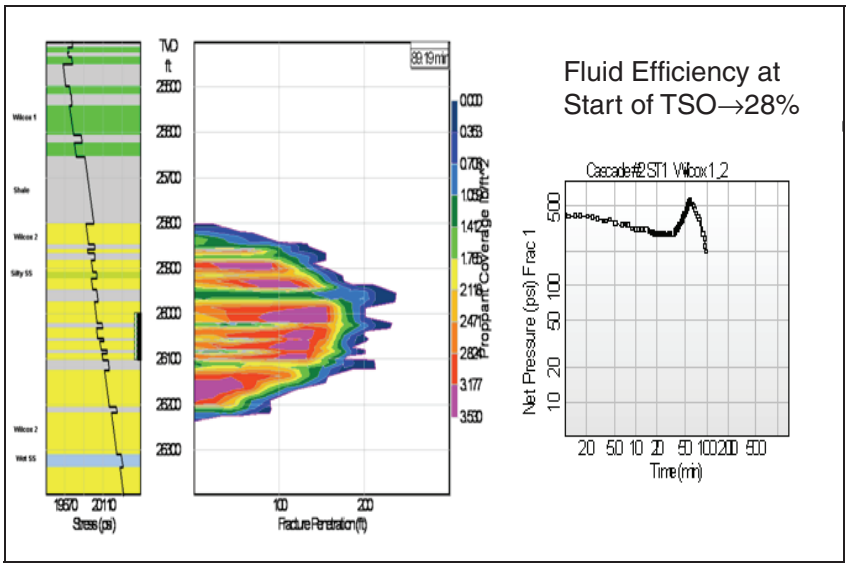

(b) Predicted Treating Pressure at 30 bbl/min

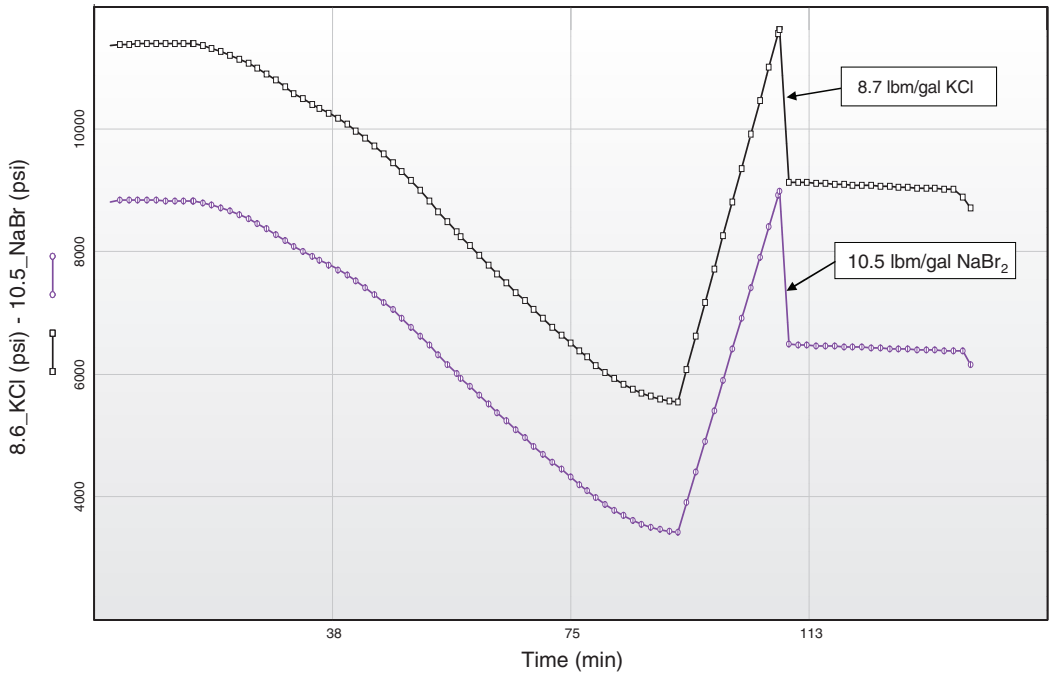

Fig. 7—Surface-pressure calculations based on Cascade offset well (7% KCl vs. 10.5 lbm/gal $NaBr_2$ frac fluid).

on the proppant-pack conductivity. This type of test is discussed by Britt et al. (2004). The proppant used to conduct the embedment tests was 20/40-US-mesh CarboHSP (Carbo Ceramics). This type of proppant was ultimately selected because of its strength and its ability to maintain good fracture conductivity under the high-confining stress environments of the Lower Tertiary formation.

The results of the study are included in Fig. 6c for a shale sample and Fig. 6d for a sand sample. The measured embedment at 12,000 psi was approximately 0.28 lbm/ft^2 in the shale and 0.21 lbm/ft^2 in the sand. A value of 0.28 lbm/ft^2 (equivalent to an incremental width change of 0.036 in.) was subsequently used for all formations in evaluating treatment designs.

Surface Treating Pressure. Given the overall gross thickness of the Wilcox formation, potential treating pump rates greater than 30 bbl/min are needed to effectively stimulate the entire reservoir. Thus, the potential for high surface treating pressure was examined. The maximum treating rate of 40 bbl/min was set as the "upper design limit" caused by the qualification of the service tool. The maximum treating pressure was set by the maximum-allowable pressure rating of the surface frac iron of 15,000 psi. Furthermore, the frac pump "kick outs" were designed to be set at 14,500 psi.

Because much of the fracture design data were developed from a Cascade exploration well, a treatment design was formulated to create a 150+ ft fracture penetration with more than 2 lbm/ft^2 bauxite coverage, as seen in **Fig. 7a.** The pump rate used for this design was 30 bbl/min. As seen in Fig. 7b, the expected treating pressure at the beginning of the frac job is 11,000 psi for 8.7-lbm/gal KCl vs. 9,000 psi for 10.5-lbm/gal $NaBr_2$. The highest treating pressure with KCl fluid is well below the maximum operating pressure of the equipment (see discussion in preceding paragraph). Because the expected moderate fluid loss (caused by the viscosity of the oil and the small expected net pressure gain during the frac job) should make it possible to design treatments using rates of 30 bbl/min or less, the need for a weighted frac fluid system was eliminated.

Fracture-Treatment Design

The basis for design developed for the Cascade exploration well (including use of high-viscosity crosslinked gel to combat fluid loss

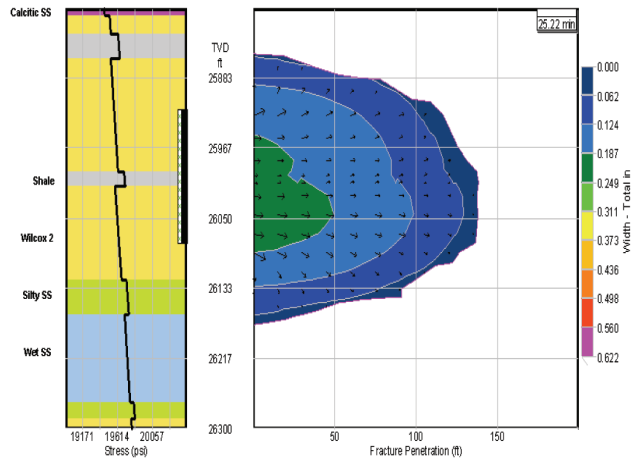

Fig. 8—Fracture growth in Well A, Stage 1 (gel injection, 25 bbl/min).

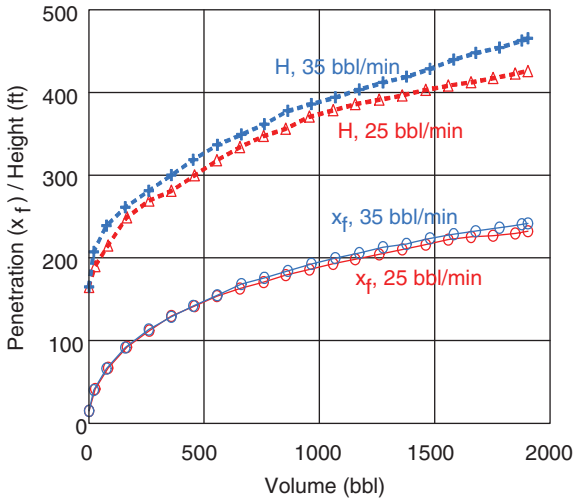

Fig. 9—Fracture-geometry predictions.

in the Wilcox 1 and the use of 20/40 US-mesh bauxite proppant) was used to create preliminary treatment designs and then to compare options (higher/lower rate, three vs. four fracs).

First, a trial perforated interval was selected and basic fracture geometry studied by simulating simple gel injections (using a gridded, planar 3D fracture simulator).

For example, consider Stage 1 in Cascade Well A. The bottommost pay targets were two Wilcox 2 sands at 25,925–26,068 ft TVD. Thus, perforations straddling these two sands might be a good approach. However, simulating a simple gel injection shows **(Fig. 8)** that the fracture has already penetrated into the water by the time it reaches the top of these two sands (after 25 minutes of pumping). Thus, this is an unacceptable option, and the price of staying away from the water may mean abandoning the bottommost Wilcox 2 sand. Thus, the perforation locations for this stage were dictated by the water at the bottom of the Wilcox.

A second selection for perforations was 25,775 to 25,905 ft TVD. Simulations were then run for injecting 80,000 gal at 25 and 35 bbl/min. The simulated growth of penetration (x_f) and height vs. volume is included in **Fig. 9.** This shows that increasing the rate had a surprisingly small effect on fracture geometry. This also shows that a practical maximum for x_f/height might be approximately 180 to 200 ft/360 to 390 ft. After that point (750 to 1,000 bbl), very large volumes are required for insignificant gains in x_f/height, and fluid efficiency is predicted to be 22%.

For the actual design, the lower rate (25 bbl/min) was selected. The pump schedule is then planned for a tip screenout (TSO) to occur after pumping 750 to 1,000 bbl, with a fracture penetration of approximately 200 ft. Additional slurry is then pumped into the fracture to increase width. To achieve this, the efficiency of 22% is used to define a first approximate schedule **(Fig. 10a).** This approach is discussed by Nolte (1986) and Martins et al. (1992). This gives a pad fraction of 67% (measured from the start of pumping pad to the start of the TSO). This first approximate schedule is then adjusted to provide the best proppant coverage. The final preliminary design and predicted fracture geometry is included in Fig. 10b.

This process was repeated for two cases. The first case included three frac stages, and the second included four. Post-frac production was then simulated with a 3D reservoir model to honor the actual geologic layering. The results are presented in **Fig. 11** as a normalized PI (BOPD/psi), with the base case being a gravel-pack completion of the entire net pay with zero mechanical skin. The normalized PI for the two cases showed that adequate formation coverage could be achieved with three fractures vs. four.

Prefrac Analysis

Prefrac testing for all treatments consisted of a gel minifrac, followed by a step-rate injection test. The crosslinked fluid would be circulated to the crossover tool, the tool would be shifted, and the minifrac

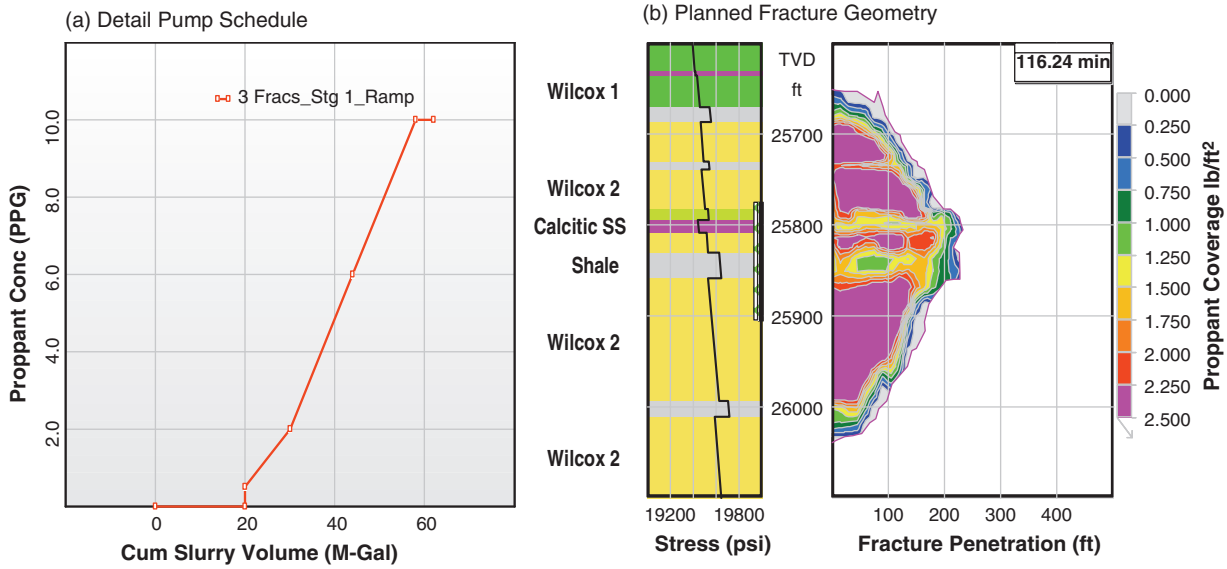

Fig. 10—Preliminary design (Well A, Stage 1).

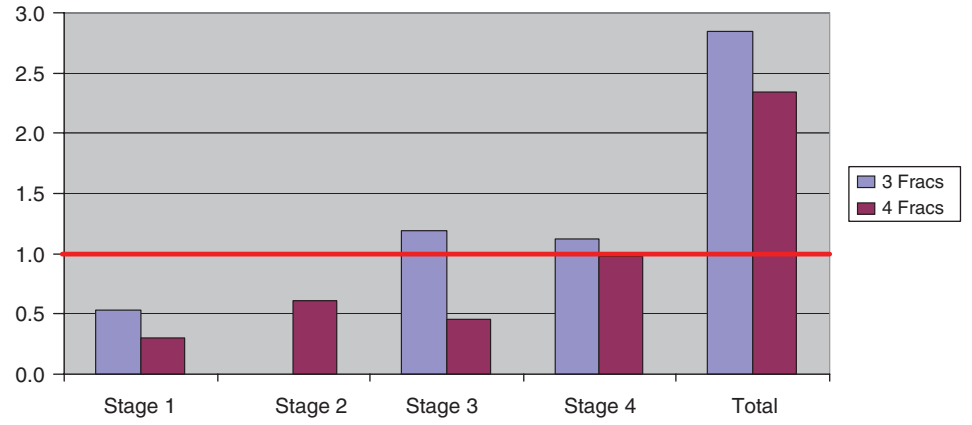

Fig. 11—Normalized PI for two completion options (Well A).

conducted by bullheading the viscous gel into the formation while displacing the work string to slickwater. After a suitable shut-in time, the step-rate test was pumped. A typical test is included in **Fig. 12.**

Closure Pressure. For prefrac testing, the first, critical step is to determine fracture-closure pressure because this is the "datum" for subsequent analysis. A step-rate injection test is useful for this purpose; by measuring the fracture-extension pressure, an absolute upper bound is placed on fracture-closure pressure. Pump rate is stepped up in small increments until fracture propagation is clearly indicated (by minimal increases in injection pressure for significant pump rate increases, as seen in **Fig. 13**). In other words, the injectivity of the well [(bbl/min)/psi] is increasing for each pump-rate increase, indicating some change in the downhole wellbore-flow condition. This presumably indicates an increase in the injection area (i.e., an increase in fracture length). In this case, the fracture is propagating at a pump rate of 5 bbl/min at an injection pressure of 21,869 psi. The intersection between the two behaviors (before and after fracture propagation) is defined as P_{EXT} [in this case, 21,780 psi at 2.8 bbl/min (0.86 psi/ft)].

This is P_{EXT} at 2.81 bbl/min; extrapolating the second (fracture-propagation line) back to zero rate gives P_{EXT} at "0" bbl/min as 21,680 psi (0.85 psi/ft as compared with an estimated overburden stress of 0.80 psi/ft). This is discussed later. A good summary of step-rate tests and pressure-decline analysis for closure pressure (as discussed later) is found in Gidley et al. (1990).

It seems logical that P_{EXT} at zero rate might equal closure pressure. There are ample anecdotal data supporting this type of analysis, and it has been discussed with data from laboratory testing by Rutqvist and Stephansson (1996). There is little theoretical justification for such a conclusion; however, we have seen many cases and discussed this matter with many who have reported similar findings; if P_{EXT} is increasing with increasing rate, then this value of 21,680 psi should be noted as a possible, approximate value for P_{CL}.

The most common approach for defining closure pressure is to analyze a pressure decline to detect the transition from "fracture linear flow" (where fluid loss from the fracture controls the decline) to "formation linear flow," (where the fracture is closed, and the elliptically shaped region of supercharged reservoir pressure begins

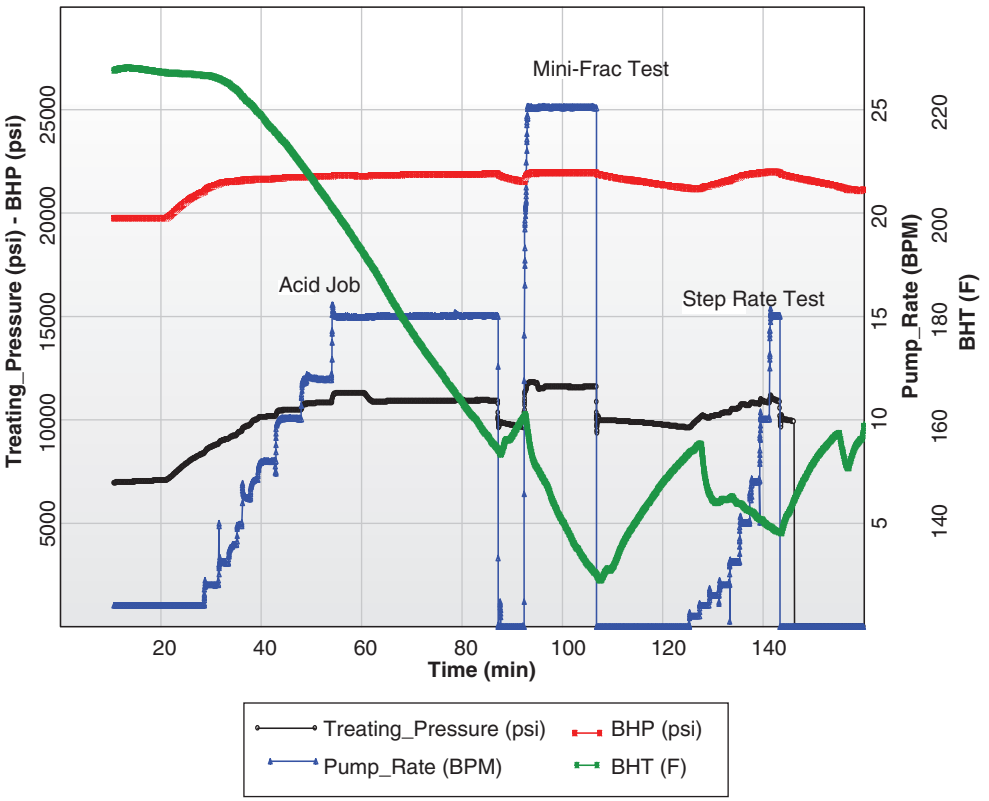

Fig. 12—Typical prefrac test procedure (Well A, Stage 2).

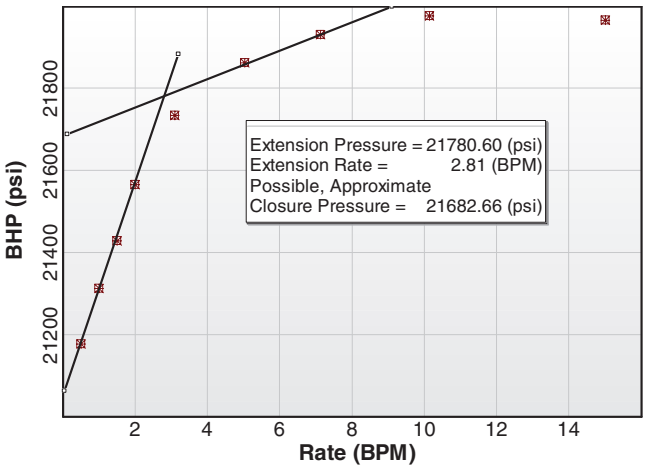

Fig. 13—Typical step-rate injection test (Well A, Stage 2).

to decline). Eventually, fracture linear flow transitions to "pseudo-radial flow" where pressure turns and begins to return to reservoir pressure. Plotting pressure vs. shut-in time, the transition will be indicated by two periods where the pressure decline is a straight line (flat derivative $dP/d\sqrt{T}$) on the $\sqrt{}$time plot. An obvious transition is seen in **Fig. 14a** at $\sqrt{T} = 1.4$ and $P = 21{,}800$ psi. However, 21,800 psi is greater P_{EXT}. Thus, this cannot be fracture closure. Beyond that, there are multiple subtle, short periods of possible linear flow, all showing the transition at approximately 21,700 psi, but no definitive value is possible.

While the $\sqrt{T}$ analysis treats the initial decline as linear flow, strictly speaking this is not true. The rigorous "straight-line" decline is pressure vs. the G-function, as discussed by Castillo (1987). As seen in Fig. 14b, the G-function results in a slightly more definitive value for P_{CL} of 21,700 psi (0.85 psi/ft). An alternative analysis of the G plot was offered by Barree and Mukherjee (1996). This was to plot $G \times dP/dG$ vs. G (Fig. 14c). When the pressure vs. G is a straight line, dP/dG will be a constant. Assuming $dP/dG = m$, then $G \times m$ will be a straight line extrapolating back to the origin ($G = 0$ and $dP/dG = 0$). The first deviation from this is taken to indicate closure (i.e., the end of the fracture linear flow). For tight rock, this can often be a powerful plot because in these cases the value of G at closure, G_{CL}, is significantly > 1. This takes the behavior of interest, the slopes of the G plot (dP/dG), and multiplies these by a value > 1, thus, magnifying the behavior changes. However, for G_{CL} < 1.0 (as for this case), this plot actually diminishes the differences, often making this a poor analysis technique for higher fluid-loss formation. However, in this case, one can still identify a possible fracture closure at 21,710 psi (Fig. 14c).

Ideally, the blue ($G \times dP/dG$) line in Fig. 14c would be a straight line from the origin to the point where the fracture closes. In this case, the $G \times dP/dG$ data drop slightly below the ideal straight line. This is where this plot is very descriptive. This "belly" is a unique indicator of fracture-height recession.

This height-recession behavior is created by the following sequence of events. First, the fracture initiates and propagates into

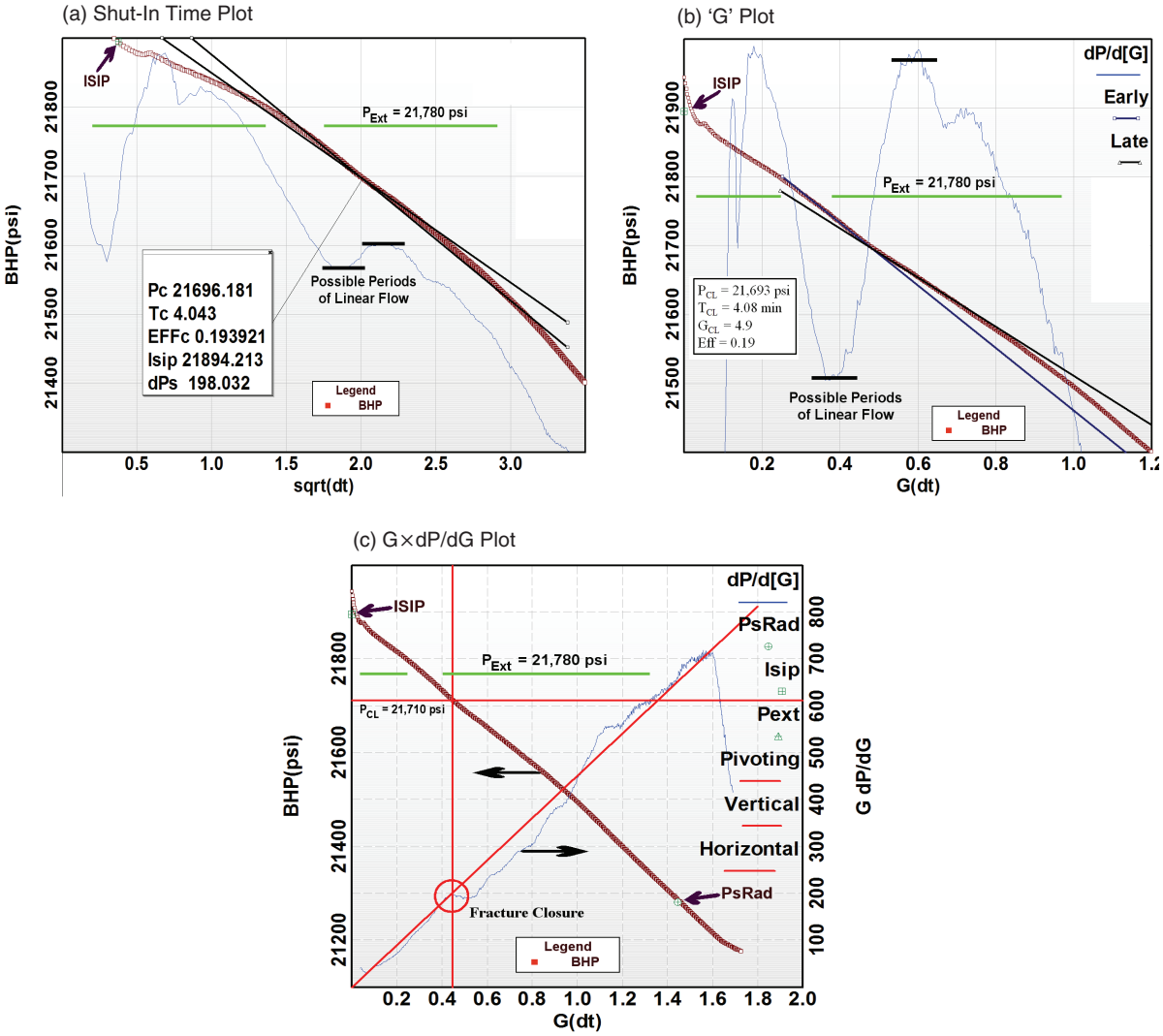

Fig. 14—Pressure-decline-analysis plots for Well A, Stage 1 (to determine P_{CL}).

TABLE 3—ESTIMATED OVERBURDEN PRESSURE			
	TVD (ft)	Pressure/Stress Gradient (psi/ft)	Incremental Pressure/Stress (psi)
Seawater	8,200	0.45	3,690
Earth	8,200 – 25,600	1.0	17,400
Total			21,090 psi
			0.83 psi/ft

the lower-stress "pay." At this point, pressure must already be greater than P_{EXT}. As the fracture grows in length, net pressure increases and the fracture may propagate up/down into adjacent higher-stress, lower fluid-loss layers (i.e., the over/underlying shale). When pumping stops, these higher-stress zones close first, forcing fluid back into the main part of the fracture. This causes a relatively slow rate of pressure decline immediately after shut-in, creating the behavior seen in Fig. 14c. However, for this case, this was surprising because radial fracture geometry was expected (i.e., minimal height confinement).

Fracture Geometry. With a clear value of P_{CL} = 21,700 psi, net pressure P_{NET} (bottomhole treating pressure minus any downhole friction minus P_{CL}) can be found. The behavior of net pressure vs. time then provides a qualitative indication of fracture geometry. However, for this case, the observed closure pressure is greater than the estimated weight of the overburden **(Table 3).** Thus, complex fracture behavior may be a possible concern. In fact, as discussed in the next paragraph, no such behavior was observed. This observation began with the absence of any significant downhole friction.

The calculated net pressure is used in the Nolte-Smith plot in **Fig. 15a.** This shows a slightly increasing trend of net pressure overall, suggesting a totally unexpected degree of height confinement. Within this slow trend are periods with net pressure increasing on a slope of 0.2 ($P_{NET} \propto \text{Time}^{0.20}$) combined with periods of falling pressure indicating height growth. Quantifying this net-pressure trend requires computer simulation. In this case, a planar fully 3D fracture-geometry model was used with the simulated net pressure included in Fig. 15b. This matches the slight upward trend in P_{NET}. Also, it captures the up/down behavior but does not exactly match the observed data. Overall, there is good agreement between the simulated data and the actual observed behavior. This provided additional indication that there was no complex fracture behavior even though the injection pressure was higher than the estimated overburden.

As noted, the height-confinement behavior was unexpected. Analysis showed this was caused by the effect of tectonic compression on the "hard streaks" (heavily calcite-cemented sands) in the formation (see logs in **Fig. 16**). Minimum in-situ stress was expected to be approximately 19,500 psi on the basis of the dipole sonic log, but measured stress was more than 2,000 psi higher. Postulating a tectonic strain of 0.002 to increase stress in the Wilcox sand to the measured level created very high confining stress in the hard streaks. This resulted in the increasing net-pressure trends seen in the Nolte-Smith plot (Fig. 15).

A possible theory for this shift in stresses would be if the formation was underlain by a massive salt that provides upward compression. This would increase the vertical stress beyond the weight of the overburden. Thus, even the elevated closure-pressure gradient of 0.85 psi/ft (OB = 0.83 psi/ft) could still represent a normal ($\sigma_{h\text{-min}} < \sigma_{h\text{-max}} < \sigma_V$) or strike-slip ($\sigma_{h\text{-min}} < \sigma_V < \sigma_{h\text{-max}}$) stress state. The resulting vertical fractures would explain the lack of operational problems.

The revised stress profile was used to history match the minifrac, with the results seen in Fig. 15b. The geometry predicted from this match is included in **Fig. 17.** The hard streaks, caused by tectonic compression, did indeed create height confinement. Later, this confinement slightly compromised the fracture treatment, limiting fracture penetration in the Wilcox 1 sand above 25,300-ft TVD and below 25,480 ft. For a later well, special care was taken in the planning to ensure that it was not necessary to fracture through a hard streak to contact all of the target pay.

Post-Frac Analysis

Post-frac analysis included net-pressure history matching, radioactive-tracer logs (the concern being can we stimulate/pack the long, 200-ft perforated intervals), and temperature trends from bottomhole memory gauges. Post-frac, bottomhole pressure (BHP) data were used to review the treatment following the prefrac test analysis. This is included (along with a treatment summary) in **Fig. 18a.** The post-frac simulation used the same geomechanical model (stress, modulus, fluid loss) as the one used for the minifrac interpretation. Given the uncertainties created by the 15-minute shut-in period (mechanical problems related to the position of the service tool to obtain a "live annulus"), bottomhole net treating pressure was nearly

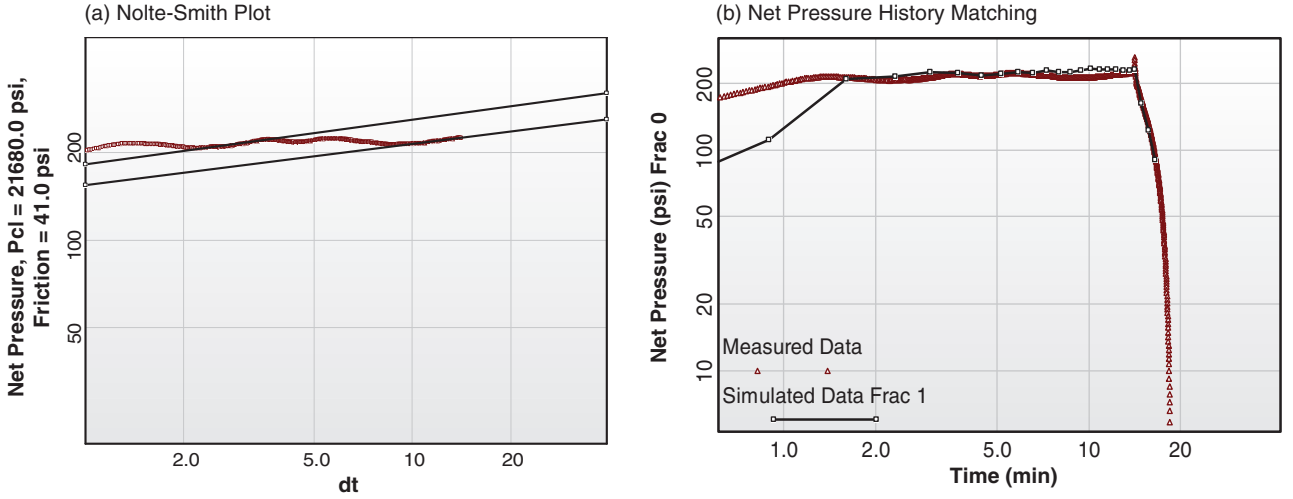

Fig. 15—Treating-pressure analysis (Well A, Stage 2).

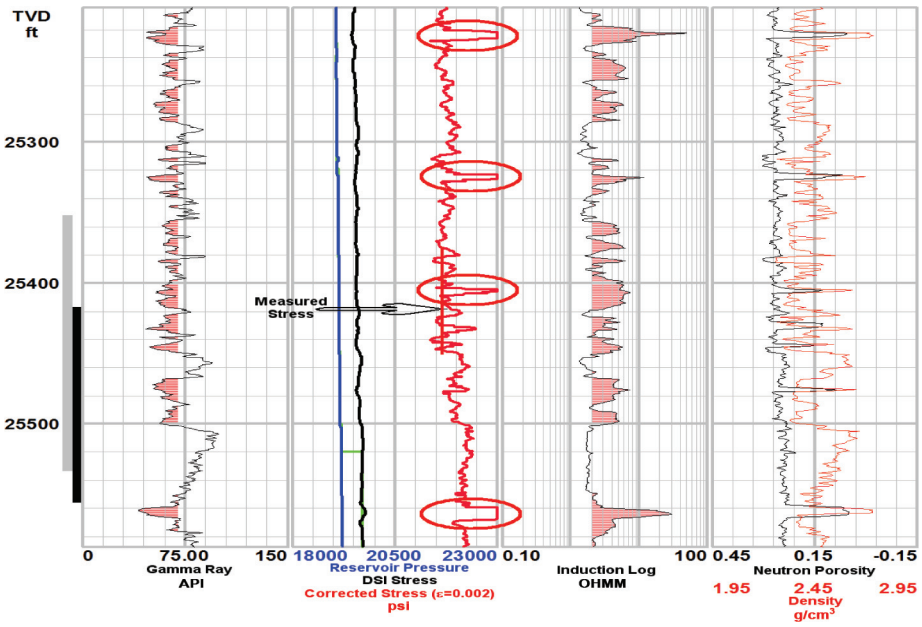

Fig. 16—Corrected stress log (Well A, Stage 2).

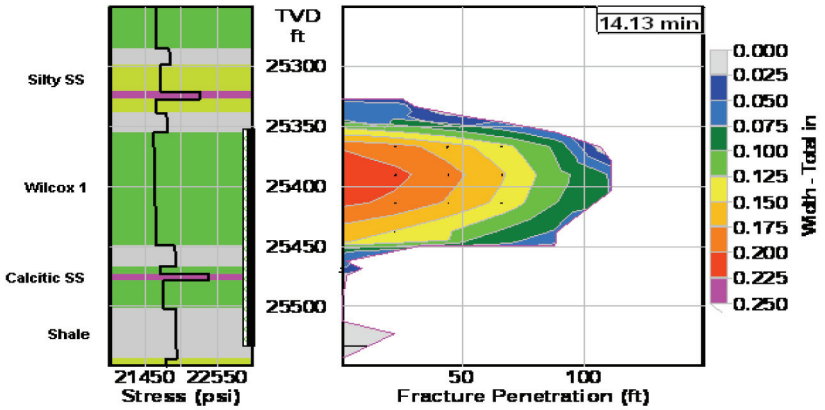

Fig. 17—Minifrac geometry (Well A, Stage 2).

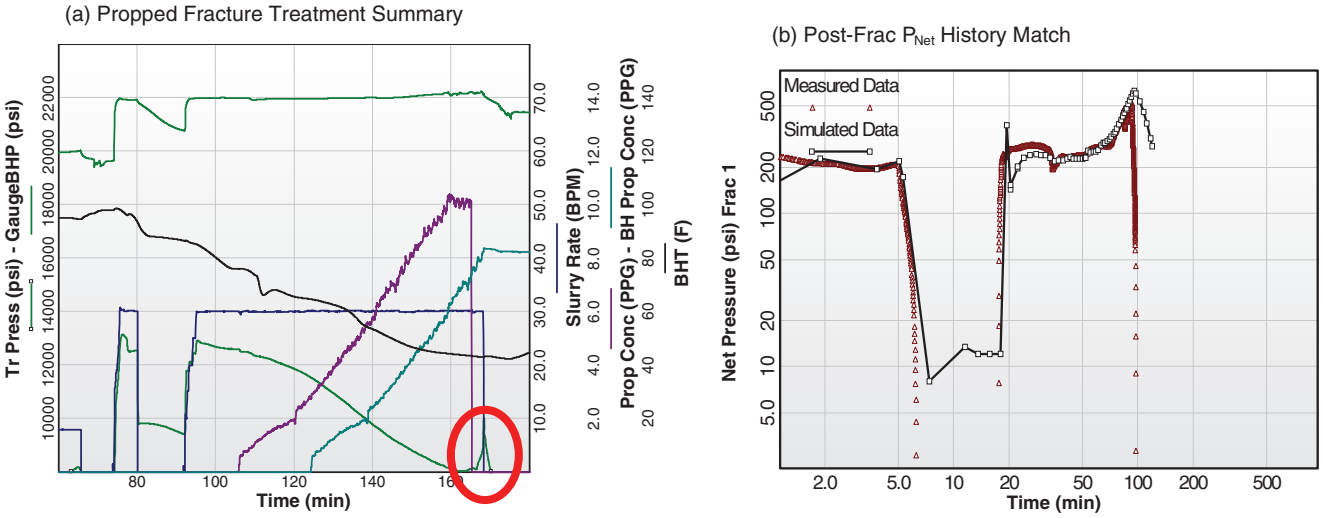

Fig. 18—Typical post-frac net-pressure analysis (Well A, Stage 2).

TABLE 4—SUMMARY OF CASCADE WELL "A" FRAC STAGES						
	Mini-Frac Fluid Eff	Vol Fluid (1,000 gal)	Vol Prop (1,000 lb_m)	Rate (bpm)	Pad Volume (as designed)	Pad Volume (as pumped)
Well A						
Stage 1	25%	53.5	103	25	32%	42%
Stage 2	12%	95	175	30	28%	36%
Stage 3	38%	72	186	30	37%	38%

equal to design predictions (Fig. 18b). However, note the surface pressure spike at approximately 168 minutes. With 8 lbm/gal on the perforations, a total, instant screenout occurred (Fig. 18a).

This same behavior also occurred on a previous treatment. With no bottomhole gauge data across the entire interval (current tool configuration allows gauges to be housed only above the top perforation), there was considerable uncertainty as to what caused the abrupt wellbore screenout. The "instantaneous screenout" behavior suggested downhole-tool problems. However, the treatment was pumped above overburden pressure; thus, a secondary fracture may have formed causing total dehydration of the slurry near the well. In any case, the treatment above (Fig. 18a) was deliberately made less aggressive (compared with the earlier treatment; see **Table 4**) in terms of increasing pad volume and designing for smaller net-pressure gain (i.e., reduced conductivity with slightly greater penetration).

The final geometry for this treatment (as compared with the initial predicted geometry in **Fig. 19a**) is included in Fig. 19b. This shows the effects of the hard streaks on the final fracture geometry. For this stage, high stresses in the hard streaks caused by compressive tectonics make it difficult to treat the thin sand (25,480 to 25,500 ft TVD), regardless of perforation placement or job size. For many other cases, the problems caused by these hard, high-stress layers can be alleviated by simply straddling these layers with the perforations (see **Fig. 20** for a post-frac analysis summary of other fracture-treatment stages).

While the net-pressure analysis (and the lack of any downhole friction, perforation friction) supports the idea of a "simple" geometry, the fact of injection pressure being greater than the estimated weight of the overburden was still a concern. This was alleviated by additional data. A radioactive-tracer scan collected when pulling the bottomhole assembly indicated proppant coverage over the entire perforated interval, again implying a vertical fracture.

Problems. Bottomhole temperature vs. time is plotted in **Fig. 21.** This shows continuous flow past the gauge throughout the treatment. Unfortunately, for the STMZ current tool configuration, the temperature/pressure gauge is always located above the top of the perforation in the "blank" pipe. Therefore, these data offer no information about downhole flow over the perforated interval. The recorded temperature did confirm much more downhole cooling than predicted. Subsequently, detailed tool examination and new tubing-movement calculations showed that the service tool had moved out of position, thus possibly causing the two total screenouts. Changes in procedures allowed the next treatment (Well A, Stage 3) to be pumped to completion, again with good agreement between predicted and measured pressure throughout. These data are discussed by Haddad et al. (2011).

Two additional failure mechanisms were analyzed to better understand the cause of the instantaneous screenouts. The first mechanism was the possibility of a late breakdown of the lower part of the perforation interval during the "sand-laden" stages of the frac job. Although this failure mechanism is highly improbable (on the basis of the detailed stress analysis and radioactive logs), it cannot be ruled out completely because of the lack of the gauge data coverage (downhole flow) across the entire perforated interval (see preceding paragraph). Additional work is under way to reconfigure the service tool to allow the installation of multiple gauge carriers across the perforation interval.

The second mechanism analyzed was the premature shearing of the crosslinked-borate fluid that would lead to a reduction in fluid viscosity and overall performance of the fluid. The reduction in fluid viscosity was analyzed as follows: (1) extra leakoff in critical areas near the wellbore and (2) limited ability to carry proppant "upwards." Approximate simulations (using a gridded, planar 3D fracture simulator) showed no potential problem with either mechanism. These simulations made no particular assumptions as to what shear rates the gel was subjected to before entering the fracture nor as to where the critical shear occurred (tools, perforations). Upon entering the fracture, the fluid was assumed to have a linear-gel rheology at wellbore temperature. This rheology was then held constant as the fluid/proppant flowed into the fracture for 20 minutes where the fluid properties were switched to the crosslink properties at the current fluid temperature/time for that fluid element.

Conclusions

On the basis of the extensive preliminary design work and post-frac analysis performed on the Cascade field, the following was concluded:

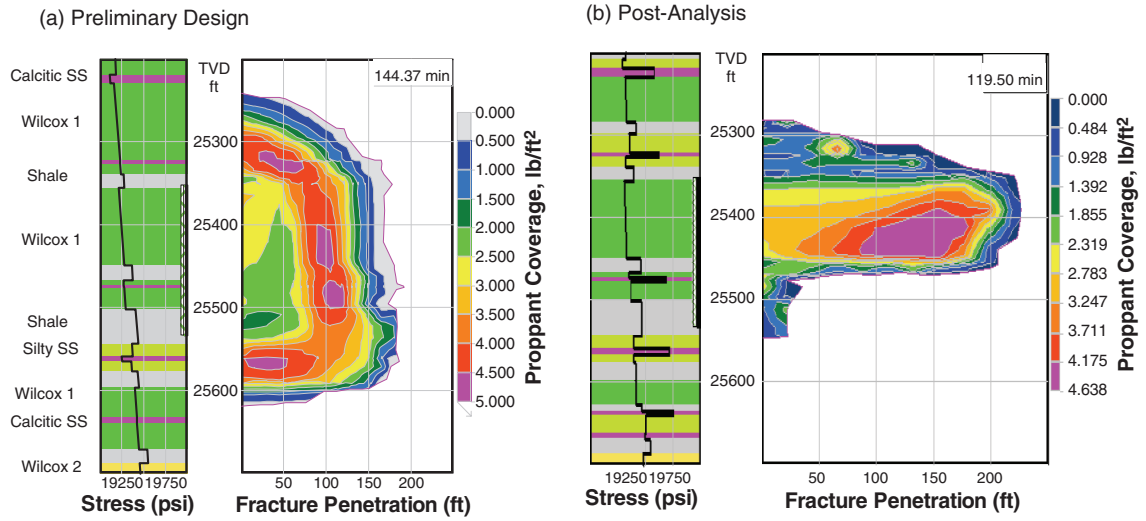

Fig. 19—Initial design vs. final fracture geometry (Well A, Stage 2).

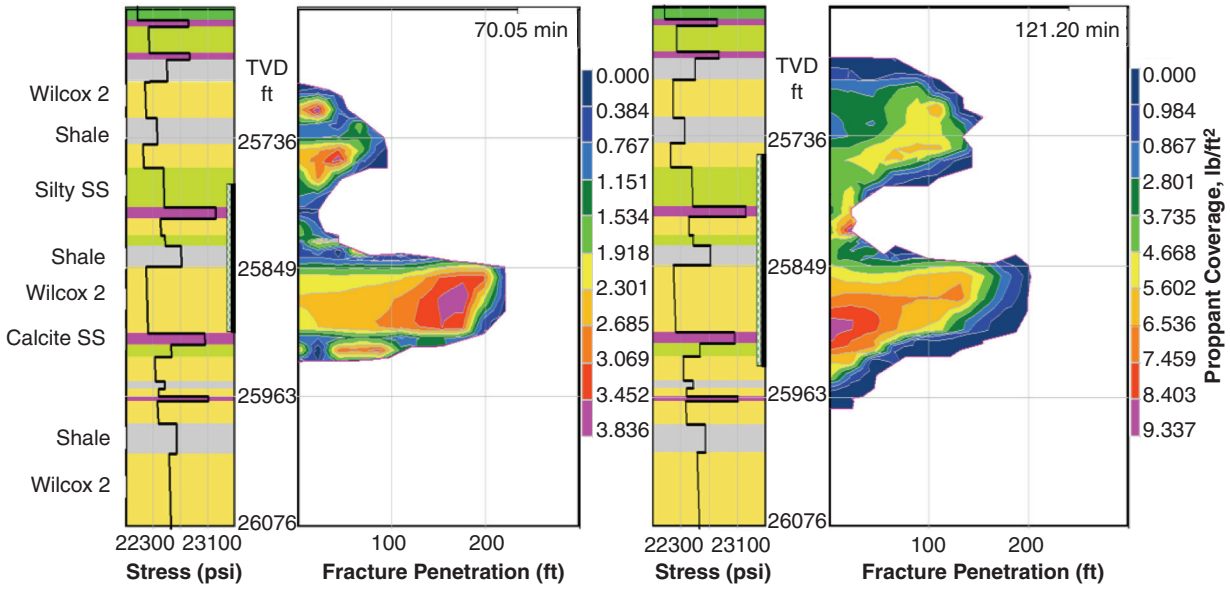

Fig. 20—Perforating across hard streaks to alleviate fracture-geometry problems (Well A, Stage 1).

- Given proper preplanning, the Lower Tertiary Wilcox formation can be stimulated effectively with a limited number of frac stages.
- On the basis of the observed stresses in the Cascade field, the fracture geometry is expected to grow beyond each perforation interval.
- Higher closure stresses were observed in the Cascade field than originally calculated. This could have been a result of higher tectonics because of salt intrusion from below.
- The closure stresses in the Cascade field exceeded the estimated overburden stress, which was not detrimental to the fracs. This conclusion was confirmed by the radioactive tracer logs that showed complete perforation coverage.
- Hard steaks in the form of calcite-cemented sands provide a height-confinement stress environment (in the presence of compressive tectonics). Properly positioning the perforation intervals (i.e., straddling the hard streaks) can provide adequate fracture coverage without adding additional frac stages.
- The total screenouts observed in Stages 1 and 2 of Well A could have been the result of the following:
  - Tool failure from frac port moving off position because of excessive cool down of work string during frac job
  - Formation failure as discussed in the preceding section

Nomenclature

C_w = fluid-loss-control coefficient of gel filter cake, ft/√min
C_T = total-fluid-loss coefficient, ft/√min
C_t = total system compressibility for the reservoir, 1/psi
dP_s = net pressure at shut-in or ISIP minus closure, psi
E = Young's modulus, psi
Eff_c = fluid efficiency from closure time
F_{CD} = dimensionless fracture conductivity
G = dimensionless time function for post-fracture pressure decline

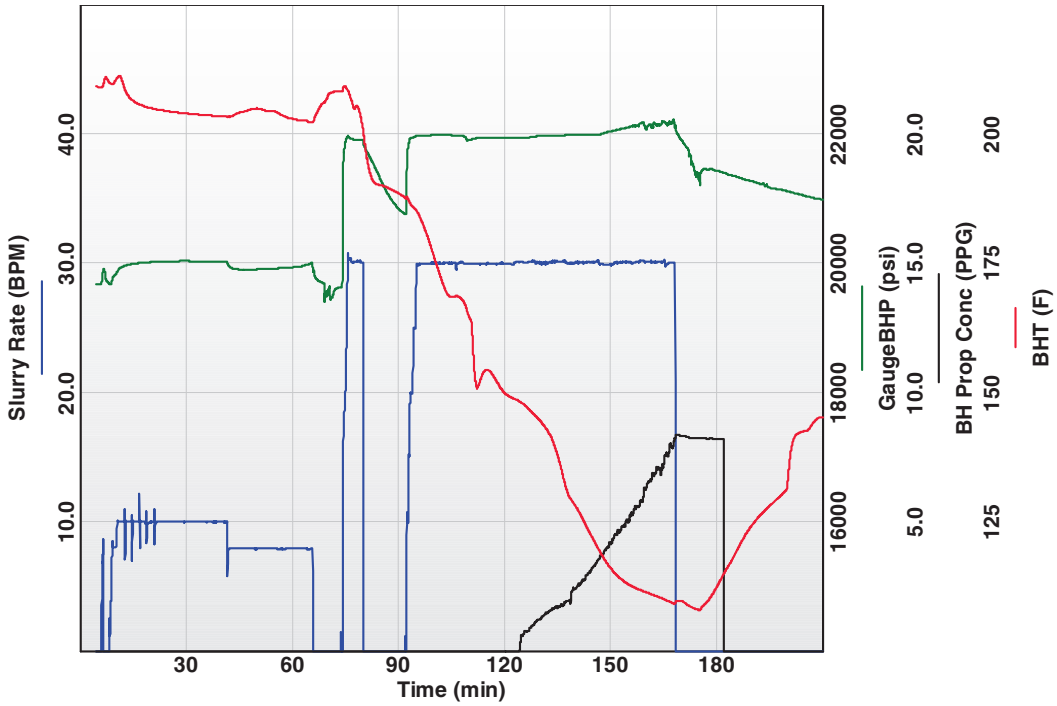

Fig. 21—BHT during treatment (Well A, Stage 2).

G_{CL} = value of G at closure
h = formation/fracture height, ft
H = fracture height, ft
H_l = fluid-loss height, ft
k = formation permeability, md
k_f = fracture permeability, md
$k\text{-}rel_{filtrate}$ = relative permeability of frac fluid leaking off to formation
K_fW = fracture conductivity, md-ft
OB = overburden-stress gradient, psi/ft
P_{CL} = fracture-closure pressure, psi
P_{EXT} = fracture-extension pressure, psi
P_e = reservoir pressure, psi
P_{NET} = net pressure, psi
$PsRad$ = pseudoradial flow
W = fracture width, ft
X_f = fracture half-length, ft
Φ = formation porosity
E = strain
σ = stress, psi
$\sigma_{h\text{-min}}$ = minimum horizontal stress or closure pressure, psi
σ_V = vertical stress or overburden, psi
$\sigma_{h\text{-max}}$ = maximum horizontal stress, psi
μ_{-oil} = oil viscosity, cp

Acknowledgments

The authors wish to thank the management of Petrobras for their support and permission to publish this work.

References

Baker Hughes. 2011. Cascade and Chinook Project (spreadsheet). Baker Hughes internal database (accessed 1 January 2011).

Barree, R.D. and Mukherjee, H. 1996. Determination of Pressure Dependent Leakoff and its Effect on Fracture Geometry. Paper SPE 36424 presented at the SPE Annual Technical Conference and Exhibition, Denver, 6–9 October. http://dx.doi.org/10.2118/36424-MS.

Britt, L.K., Smith, M.B., Haddad, Z., and Lawrence, P. 2006. A Multi-Disciplinary Approach to Hydraulic Fracturing in the South Texas, Wilcox Formation. Paper SPE 102226 presented at the SPE Annual Technical Conference and Exhibition, San Antonio, Texas, USA, 24–27 September. http://dx.doi.org/10.2118/102226-MS.

Britt, L.K., Smith, M.B., Haddad, Z., Reese, J., and Kelly, P. 2004. Rotary Sidewall Cores—A Cost Effective Means of Determining Young's Modulus. Paper SPE 90861 presented at the SPE Annual Technical Conference and Exhibition, Houston, 26–29 September. http://dx.doi.org/10.2118/90861-MS.

Castillo, J.L. 1987. Modified Fracture Pressure Decline Analysis Including Pressure-Dependent Leakoff. Paper SPE 16417 presented at the Low-Permeability Reservoirs Symposium, Denver, 18–19 May. http://dx.doi.org/10.2118/16417-MS.

Cunha, J.C.S., Moreira, O.M.M., Azevedo, G.H., Pereira, B.M., and Rocha, L.A.S. 2009. Challenges on Drilling and Completion Operations of Deep Wells in Ultra-Deepwater Zones in the Gulf of Mexico. Paper SPE 125111 presented at the SPE Annual Technical Conference and Exhibition, New Orleans, 4–7 October. http://dx.doi.org/10.2118/125111-MS.

Gidley, J.L., Holditch, S.A., Nierode, D.E., and Veatch, R.W. Jr. 1990. *Recent Advances in Hydraulic Fracturing*, No. 12. Richardson, Texas: Monograph Series, SPE.

Gil, I.R., Smith, M.B., Haddad, Z. et al. 2007. "Super Height Growth"—Strange Surface Pressures and Refrac Potential. Paper SPE 106083 presented at the SPE Hydraulic Fracturing Technology Conference, College Station, Texas, USA, 29–31 January. http://dx.doi.org/10.2118/106083-MS.

Haddad, Z.A., Smith, M.B., de Moraes, F.D., and Moreira, O.M.M. 2011. The Design and Execution of Frac Jobs in the Ultra Deepwater Lower Tertiary Wilcox Formation. Paper SPE 147237 presented at the SPE Annual Technical Conference and Exhibition, Denver, 30 October–2 November. http://dx.doi.org/10.2118/147237-MS.

Halliburton Energy Services. 2011. Fracture treatments, historical data (spreadsheet). Halliburton internal database (accessed 1 January 2011).

Lacy, L.L. 1997. Dynamic Rock Mechanics Testing for Optimized Fracture Designs. Paper SPE 38716 presented at the SPE Annual Technical Conference and Exhibition, San Antonio, Texas, USA, 5–8 October. http://dx.doi.org/10.2118/38716-MS.

Lestz, R.S., Clarke, J.N., Plattner, D., and Byrd, A.C. 1999. Perforating for Stimulation: An Engineered Solution. Paper SPE 56471 presented at the SPE Annual Technical Conference and Exhibition, Houston, 3–6 October. http://dx.doi.org/10.2118/56471-MS.

Martins, J.P., Leung, K.H., Jackson, M.R., Stewart, D.R., and Carr, A.H. 1992. Tip Screenout Fracturing Applied to the Ravenspurn South Gas Field Development. *SPE Prod Eng* **7** (3): 252–258. SPE-19766-PA. http://dx.doi.org/10.2118/19766-PA.

Meyer, B.R. and Jacot, R.H. 2005. Pseudosteady-State Analysis of Finite-Conductivity Vertical Fractures. Paper SPE 95941 presented at the SPE Annual Technical Conference and Exhibition, Dallas, 9–12 October. http://dx.doi.org/10.2118/95941-MS.

Moraes, F.D., Moreira, O., Ogier, S., Haddad, Z., and Shipley, J. 2010. Well Completion Operations in Cascade and Chinook Fields—Ultra Deep Water Challenges in the Gulf of Mexico. Paper IBP 3310 presented at the Rio Oil & Gas 2010 Expo and Conference, Rio de Janeiro, 17–20 September.

Nolte, K.G. 1986. Determination of Proppant and Fluid Schedules From Fracturing-Pressure Decline. *SPE Prod Eng* **1** (4): 255–265. SPE-13278-PA. http://dx.doi.org/10.2118/13278-PA.

Ogier, K.S., Haddad, Z.A., Moreira, O.M.M., de Moraes, F.D., and Shipley, J. 2011. The World's Deepest Frac-Pack Completions Utilizing a Single-Trip, Multi-Zone System: A Gulf of Mexico Case Study in the Lower Tertiary Formation. Paper SPE 147313 presented at the SPE Annual Technical Conference and Exhibition, Denver, 30 October–2 November. http://dx.doi.org/10.2118/147313-MS.

Rutqvist, J. and Stephansson, O. 1996. A cyclic hydraulic jacking test to determine the in situ stress normal to a fracture. *International Journal of Rock Mechanics and Mining Sciences & Geomechanics Abstracts* **33** (7): 695–711. http://dx.doi.org/10.1016/0148-9062(96)00013-7.

Sanders, W., Baumann, C.E., Williams, H.A.R. et al. 2011. Efficient Perforation Of High-Pressure Deepwater Wells. Paper OTC 21758 presented at the Offshore Technology Conference, Houston, 2–5 May. http://dx.doi.org/10.4043/21758-MS.

Smith, M.B., Bale, A.B., Britt, L.K., Klein, H.H., Siebrits, E., and Dang, X. 2001. Layered Modulus Effects on Fracture Propagation, Proppant Placement, and Fracture Modeling. Paper SPE 71654 presented at the SPE Annual Technical Conference and Exhibition, New Orleans, 30 September–3 October. http://dx.doi.org/10.2118/71654-MS.

Ziad Haddad established FOI Technologies in 2010 as a deepwater consulting company. Before that, he worked for Pennzoil Production Company and Devon Energy Corporation as a Well Engineering Advisor on numerous high-profile domestic and international projects onshore and offshore. He has spent the last 15 years working in the design and implementation of all aspects of well completions with emphasis in the field of hydraulic fracturing. Most recently, he has been working with Petrobras on developing its ultra deepwater Lower Tertiary Cascade and Chinook Project. He holds a BS degree in petroleum and natural gas engineering from Pennsylvania State University. He has authored several technical papers and is an active member of SPE.

Michael Berry Smith works with NSI Technologies and specializes in rock mechanics, well completions, and hydraulic fracturing. He has experience with major operators and as an independent consultant. He holds degrees in mechanical engineering from Rice University. He has authored numerous patents and technical papers and received the SPE Lester C. Uren award for his technical contributions to hydraulic fracturing.

Flavio Dias de Moraes is a senior well engineer advisor working on ultradeepwater well drilling and completion design. He has worked as a technical consultant in well completions and material science and has had several management assignments, including asset well construction manager and well engineering manager at Petrobras R&D Center. Since 2007, he's been the well engineering manager for Petrobras America, Inc., and was responsible for the well design for Cascade and Chinook fields in the lower tertiary Gulf of Mexico. He holds two patents, has published numerous papers, and has participated in various SPE organized events. He holds a PhD degree in petroleum engineering from the University of Tulsa, an MSc degree in material science from COPPE/UFRJ Brazil, and a BS degree in mechanical engineering from IME Brazil.